Cross Sections of the ^{36}Ar(d,α)^{34m}Cl, ^{40}Ar(d,α)^{38}Cl and ^{40}Ar(d,p)^{41}Ar Nuclear Reactions below 8.4 MeV

J W Engle[1,*], **G W Severin**[1,*], **T E Barnhart**[1], **L D Knutson**[2], and **R J Nickles**[1]

[1]University of Wisconsin Department of Medical Physics

[2]University of Wisconsin Department of Physics

Abstract

We have measured the cross section for production of the medically interesting isotope ^{34m}Cl, along with ^{38}Cl and ^{41}Ar, using deuteron bombardments of ^{36}Ar and ^{40}Ar below 8.4 MeV. ALICE/ASH analytical codes were employed to determine the shape of nuclear excitation functions, and experiments were performed using the University of Wisconsin tandem electrostatic accelerator to irradiate thin targets of argon gas.

Keywords

^{34m}Cl; ^{38}Cl; PET

Introduction

Production of ^{34m}Cl (ß$^+$ = 55%, t$_{1/2}$ = 32.0m) by deuteron bombardment of ^{36}Ar gas was recently reported (Engle *et al*., 2011a). Thick target irradiations of ^{36}Ar gas and subsequent separation techniques yield sufficient ^{34m}Cl for use in medical imaging experiments, and irradiations of ^{nat}Ar gas provide an inexpensive chemical surrogate, ^{38}Cl (ß$^-$ = 100%, t$_{1/2}$ = 37.2m), for developmental work. The prevalence of chlorine compounds from anthropogenic and natural sources offers varied and fertile ground for scientific explanation with their radiolabeled counterparts, and many known compounds' biological or toxicological effects result from chlorination in functional positions (Engle *et al*., 2011b).

The radioisotopes of chlorine have a production history dating to the 1960's using a variety of incident particles and energies. Though a variety of chalcogen targets have been used to produce ^{34m}Cl, only alpha irradiations of sulfur targets with natural isotopic abundance have been used routinely or produced radioisotope in sufficient quantity and chemical utility for positron emission tomography (PET) imaging (Takei *et al*., 2007). While reported thick target yields for sulfur irradiations exceed those we have measured for deuteron bombardments of argon, accelerator targetry using sulphur and its compounds is problematic due to the element's poor thermal and electrical conductivity, low melting point, and tendency to sublime (Abrams *et al*., 1984; Nagatsu *et al*., 2008). Irradiations of argon gas, by contrast, offer the prospect of clean separation chemistry and facile ^{36}Ar recovery using

*J W Engle and G W Severin contributed equally to this work.

cryotrapping techniques, which, at Wisconsin, average >99.5% over more than 40 cycles. Williams and Irvine (1963) studied the production of ^{38}Cl by (d,α) above 10.5 MeV, but data for radiochlorine production below 10 MeV, near energies typical of modern medical cyclotrons, are absent from available literature. Knowledge of the nuclear excitation function would permit targetry optimization with implications for subsequent radiochemical syntheses. Only ^{41}Ar (β$^-$ = 100%, $t_{1/2}$ = 109.6m) is produced as a radiocontaminant during irradiation of natural argon gas. Previously, Fitz *et al.* (1968), Kashy *et al.* (1961), and Carvallo *et al.* (1975) studied the angular distribution of secondary particles and the excitation states of produced ^{41}Ar at 11.6 MeV, 7.5 MeV, and below the Coulomb barrier, respectively, but did not characterize the (d,p) excitation function.

Methods

The ^{36}Ar(d,α)^{34m}Cl, ^{40}Ar(d,α)^{38}Cl and ^{40}Ar(d,p)^{41}Ar nuclear reactions were analytically computed and measured. ALICE-ASH is an advanced and modified version of the original ALICE code used for the analytical computation of excitation functions, as well as energy and angular distribution of secondary particles in nuclear reactions induced by nucleons with energies below 300 MeV (Broeders *et al.*, 2006). Computed results of the ALICE-ASH code runs compared favorably with well-described deuteron reactions (e.g. ^{60}Ni(d,n)^{61}Cu) but poorly with well-described (d,α) reactions (e.g. ^{20}Ne(d,α)^{18}F). The latter machine's beam profile is especially suited to cross section measurements involving small targets of enriched isotopes.

Argon gas targets were made from 0.635 cm OD, 0.159 cm ID steel tubes, cross-drilled with 0.476 cm holes sealed by two epoxied 12.5 um aluminum foil windows (Goodfellow, UK). Tubes were approximately 10 cm in length to accommodate closure valves, fittings for filling the targets, and small-volume bourdon gauges for continuous monitoring of target gas pressure. Targets were filled in an evacuated (120 mbar) container after themselves being evacuated at 20.3°C to avoid stressing the foils with negative pressure. Fill pressures were measured using an Omegadyne (Ohio) PX309 pressure transducer. The transducer was calibrated from 1 to 7 bar between -15.5 and 79.4°C with manufacturer-supplied uncertainty of ± 7 mbar at atmospheric pressure. Initial bourdon gauge and transducer pressures were recorded and, with adjustments for ambient temperature, used to monitor the quantity of target gas irradiated in each run. Pressure in all targets showed no measurable change over an irradiation period spanning 8 months. Cryotrapping recovered target gas when filling targets with ^{36}Ar gas as described previously (Engle *et al.*, 2011a).

The targets containing either ^{nat}Ar gas or ^{36}Ar gas (99.993%, Isoflex, San Francisco) were inserted into the beamline of the University of Wisconsin Physics Department's tandem electrostatic accelerator. Tantalum slits collimated the deuteron beam to 1 mm^2 at 4 cm in front of the target, as shown in Figure 1 below. After passing through the gas and both foils, the beam entered a -200 V cylindrical suppressor tube 4 cm behind the target to eliminate electrons produced by beam interactions in the target and permit accurate integration of irradiation currents hitting the molybdenum beam stop. Straightforward Stopping and Range of Ions in Matter (SRIM/TRIM) simulations confirm that fewer than 0.1% of deuterons fail to reach the suppressor at 3.0 MeV incident energy and permit estimation of uncertainty in time-integrated beam currents; these results are shown, along with a target schematic, in Figure 1 below (Ziegler *et al.*, 2008). SRIM calculations yield an energy loss in the target chamber of 120 keV for a 4 MeV incident deuteron.

The targets were irradiated with 200 to 600 nA of 3 to 8 MeV deuterons for 10 to 30 min. Current and dome voltage were continuously monitored and logged by an in-house Labview code at 1 kHz. Logged variation (as RMS deviation of this signal) in dome voltage was

weighted by beam current for calculation of excitation functions. Deuteron energy after the first aluminum foil was computed using range tables (Ziegler *et al.*, 2008) and used to correct logged and averaged dome energy measurements (see Figure 2 below).

Following irradiation, targets were assayed by γ-spectroscopy using a 66 cm^3 high-purity germanium (HPGe) detector (Canberra model GC1519, FWHM @ 1333 keV = 4.6 keV). For irradiations of the natural argon target, regions of interest (ROIs) were drawn over the 2.167 and 1.642 MeV peaks of ^{38}Cl and the 1.293 MeV peak of ^{41}Ar. For the separated ^{36}Ar target, the 2.128 and 1.176 MeV γ emissions of ^{34m}Cl were used. No contaminant γ lines other than those from ^{27}Al(d,p)^{28}Al (β$^-$ = 100%, t$_{1/2}$ = 2.25 min, 1.78 MeV γ) were observed when counting irradiated ^{36}Ar targets. Spectra with 20 sec length were collected for 50 min using an ASPEC multichannel analyzer (MCA) and the Maestro-32 γ spectroscopy software suite (Ortec, Oak Ridge, TN).

The number of $^{34m/38}$Cl and ^{41}Ar nuclei at the end of irradiation was determined from known mean lifetimes and the intercept of an exponential fit of photopeak sums as a function of time (see example in Figure 3 below). Counter dead time and photopeak contribution from pileup were determined with a 10.00 Hz pulser input to the HPGe amplifier located at 2.35 MeV, whose variance over each run permitted estimation of the error in reported dead time, rejecting out of these only spectra contaminated by ^{28}Al decay emissions. Individual photopeak backgrounds were estimated and subtracted using averaged ROIs immediately above and below the photopeak area.

During irradiation, the change in the number of beam-produced nuclei, *dN*, in a given time *dt* is given by

$$dN = Rdt - \lambda Ndt,$$

where *R* is the rate at which the isotope is being produced and λ is the decay constant. *R* can further be defined by the expression

$$R = \sigma ITK,$$

where *σ* is the cross section for the isotope's production, *I* is the beam current, *T* is the target thickness, and *k* is a unit-driven constant. Proceeding with the indicated numerical integration over *dt*, using the logged record of beam current for *I(t)* gives a value which can be compared to the value of *N* from a characteristic peak in the collected gamma spectrum with *σ* as a fit parameter, allowing estimation of the uncertainty in the reported *σ*.

Results

The following Figures (4 - 6) and Tables (1 and 2) show measured and computed cross sections from ALICE-ASH results for the three nuclides of interest along with previously reported values, when available, at nearby energies for comparison. Computed curves suggested excitation functions whose peaks were energetically below the range of previously reported values (for ^{38}Cl) and near energies achievable on modern, low-energy cyclotrons and the University of Wisconsin's tandem electrostatic accelerator. Only statistical errors are shown in plots. Uncertainties in scale factors with anticipated uniform effects (e.g. beam current integration, bias in target pressure and thickness measurements, HPGe detector efficiency, etc…) are not shown in the plots below.

Discussion

Several sources of statistical error contribute to the uncertainty in these data. Random error in measured values of target pressure ($\pm$ 3 mbar) causes reported results to vary by <1%. HPGe γ-spectroscopy entails the introduction of statistical error from counting, pileup, dead time, and background subtraction. Poisson-distributed error in background- and deadtime-corrected photopeaks weights the (χ^2 minimization, single free parameter) fit of photopeak sums in 20 sec spectra used to determine activity at the end of irradiation, allowing estimation of error in the fit from known residuals. A typical correction from pulser and deadtime data altered photopeak counts in a single 20 sec spectra by 2 $\pm$ 1% (mean $\pm$ SD) prior to fitting. Positioning reproducibility during counting of $\pm$ 1 mm produces variability of $\pm$ 0.5% in detector efficiencies, a factor of 10 less than the uncertainty in the detector efficiency for ^{34m}Cl's principle gamma at 2.128 MeV.

Systematic scale factor errors are more difficult to estimate. Tests of beam integration electronics' accuracy using known sources as input yield logged currents accurate to within $\pm$ 0.01%, well inside the precision of the logged signal and in agreement with independent, parallel electrometer measurements (Keithley, Ohio). The assumption of point-source-like geometry for counting ^{34m}Cl and ^{38}Cl is justified by previous work suggesting unity sticking probability of radiochloride's adherence to metallic surfaces inside accelerator targets (Engle *et al.*, 2011a). HPGe detector efficiencies were computed using calibrated sources in an identical geometric position to further account for this error. However, this same assumption is much less valid for ^{41}Ar, which can be expectedly to diffuse throughout the target and the dead volume of the bourdon gauge over time. Collimated assays of targets conducted 4-6 hours post-irradiation show only 16 $\pm$ 3% of produced ^{41}Ar located in the aluminum-windowed thru-hole, with the balance of the inert product distributed in the Bourdon gauge. Reported error bars reflect the less than 5% mismatch, estimated geometrically, between point source and actual counting efficiency in the case of this source distribution of ^{41}Ar. Beam heating of the argon gas effectively thins the target even at sub-microamp irradiation currents and artificially lowers calculated cross sections. Using standard equations for conduction and convection, this effect causes systematic underestimation of results by less than 6%. We estimate total error in the measurement to be less than 9% using the effects discussed above.

Measured data for ^{34m}Cl and ^{38}Cl differ from the excitation functions returned by ALICE-ASH computations. Notably, the measured ^{38}Cl cross section appears to peak 2-3 MeV below computational results. Predicted decline in the ^{41}Ar cross section at decreasing energies was not observed at the lowest incident energy achievable in this experiment, perhaps because of the difficulty of describing deuteron-induced multiple nucleon-pickup reactions using computational methods. Lower energies were attempted, but these attempts resulted in unstable dome voltages and deuteron currents. Measured data do appear to agree with extrapolated literature values for the cross section of ^{38}Cl, though the energy limitations of the University of Wisconsin tandem electrostatic accelerator prevent acquisition of overlapping data points near 10.5 MeV (Williams and Irivine, 1963).

Calculated thick target yields using the measured cross section are higher than previously measured production yields trapping $^{34m/38}$Cl on foil liners in 60 ml targets (5.2 $\pm$ 0.3 vs 1.8 $\pm$ 0.2 mCi/uA for ^{34m}Cl and 4.6 $\pm$ 0.3 vs 1.4 $\pm$ 0.2 mCi/uA for ^{38}Cl at the end of saturated bombardment) (Engle *et al.*, 2011a). This strongly suggests the loss of radiochloride from trapping on exposed metal surfaces in production targets; losses might be recovered by rinsing these targets post-irradiation, offering the promise of a factor of two in yield for productions of ^{34m}Cl for preclinical imaging studies.

Conclusions

The reported cross sections for ^{34m}Cl and ^{38}Cl establish that low energy cyclotrons are well matched to the optimum energy for these isotopes' production by deuteron irradiation. We have measured the cross section for the production of ^{34m}Cl, ^{38}Cl, and ^{41}Ar using deuteron bombardments of ^{36}Ar and ^{40}Ar below 8.4 MeV. These data reveal the possibility of increased production yields of the medically interesting isotope ^{34m}Cl and describe the nuclear excitation functions of three isotopes of interest in a previously uncharacterized energy window.

Acknowledgments

References

Abrams DN, Knaus EE, Wiebe LI, Helus F, Maier-Borst W. Production of ^{34m}Cl from a gaseous hydrogen sulfide target. International Journal of Applied Radiation and Isotopes. 1984; 35:1045–1048.

Takei M, Nagatsu K, Fukumura T, Suzuki K. Remote control production of an aqueous solution of no-carrier-added ^{34m}Cl- via the ^{32}S(α,pn) nuclear reaction. Journal of Applied Radiation and Isotopes. 2007; 65:981–986.

Broeders, CHM.; Konobeyev, AY.; Korivin, YA.; Lunev, VP.; Blann, M. ALICE/ASH Pre-compound and Evaporation Model Code System for Calculation of Excitation Function Energy and Angular Distributions of Emitted Particles in Nuclear Reactions at Intermediate Energies. Forschungszentrum Karlsruhe GmbH, Karlsruhe No 7183. 2006. Retrieved from <http://bibliothek.fzk.de/zb/berichte/FZKA7183.pdf>

Cavallaro S, Corleo G, Cunsolo A, Foti A, Giambruno S, Toro MD, Pappalardo G. The ^{41}Ar(d,p)^{41}Ar reaction at deuteron energies below the coulomb barrier. Il Nuovo Cimento. 1975; 28(1):12–20.

Engle JW, Barnhart TE, DeJesus OT, Nickles RJ. Production of 34mCl and ^{38}Cl via the (d,α) reaction on ^{36}Ar and ^{nat}Ar gas at 8.4 MeV. Journal of Applied Radiation and Isotopes. 2011a; 69:75–79.

Engle JW, Barnhart TE, Severin GW, Nickles RJ. The unrealized potential of ^{34m}Cl for radiopharmaceutical research with PET. Current Radiopharmaceuticals. 2011b; 4(2):102–108.

Fitz W, Jahr R, Santo R. The (d,p) and (d,t) reactions on ^{38}Ar and ^{40}Ar. Nuclear Physics A. 1968; 114:392–400.

Kashy E, Hoogenboom AM, Buechner WW. Level structure of Ar-41 from the Ar-40(d,p)Ar-41 reaction. Physical Review. 1961; 124:1917–1922.

Nagatsu K, Fukumura T, Takei M, Szelecsenyi F, Kovacs Z, Suzuki K. Measurement of thick target yields of natS(α,x)34mCl nuclear reaction and estimation of its excitation function up to 70 MeV. Nuclear Instruments and Methods in Physics Research B. 2008; 266:709–713.

Williams DC, Irvine JW. Excitation functions and thick-target yields: Zn+d and Ar^{40}(d,alpha). Physical Review. 1963; 130:265–271.

Ziegler, JF.; Biersack, JP.; Ziegler, MD. The stopping and range of ions in matter. Lulu Press Co.; Morrisville, NC: 2008.

Highlights

➤ ALICE-ASH computed cross sections
for $^{36}Ar(d,\alpha)^{34m}Cl$, $^{40}Ar(d,\alpha)^{38}Cl$, $^{40}Ar(d,p,)^{41}Ar$

➤ Measured cross sections for $^{36}Ar(d,\alpha)^{34m}Cl$, $^{40}Ar(d,\alpha)^{38}Cl$, $^{40}Ar(d,p,)^{41}Ar$

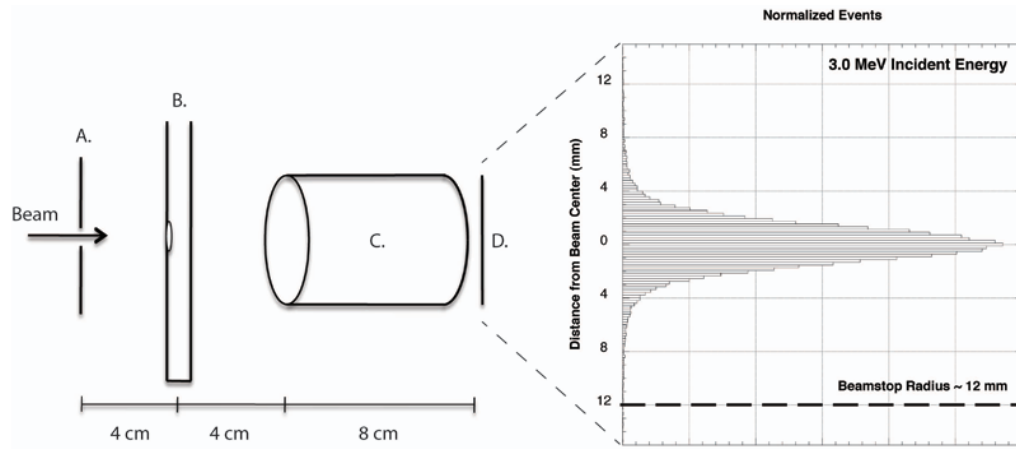➤ Deuteron irradiations < 9 MeV are optimal for ^{34m}Cl production for PET

Figure 1.
Irradiation geometry, showing A) x/y slits limiting beam to 1 mm^2, B) target containing argon gas, C) -200 V suppressor, D) beam stop, and the radial distribution of deuterons at the beam stop for various incident energies from TRIM calculations. Dimensions are approximate.

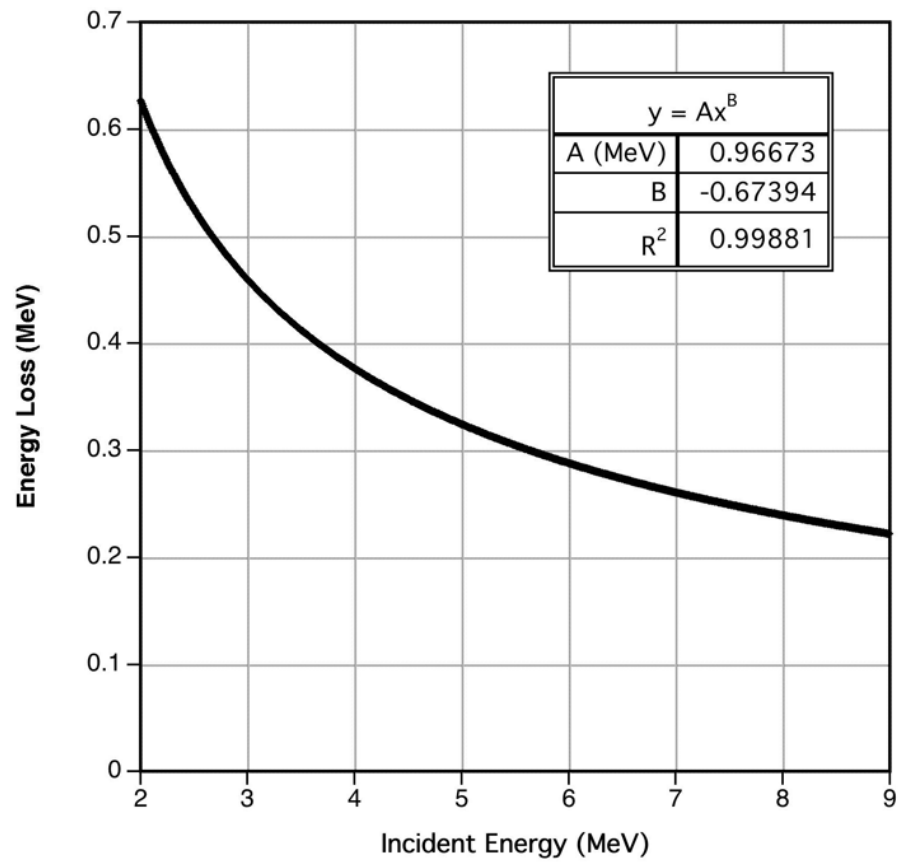## Deuteron Energy Loss (MeV) in 12.5um Al foil vs Incident Energy (MeV)

Figure 2.
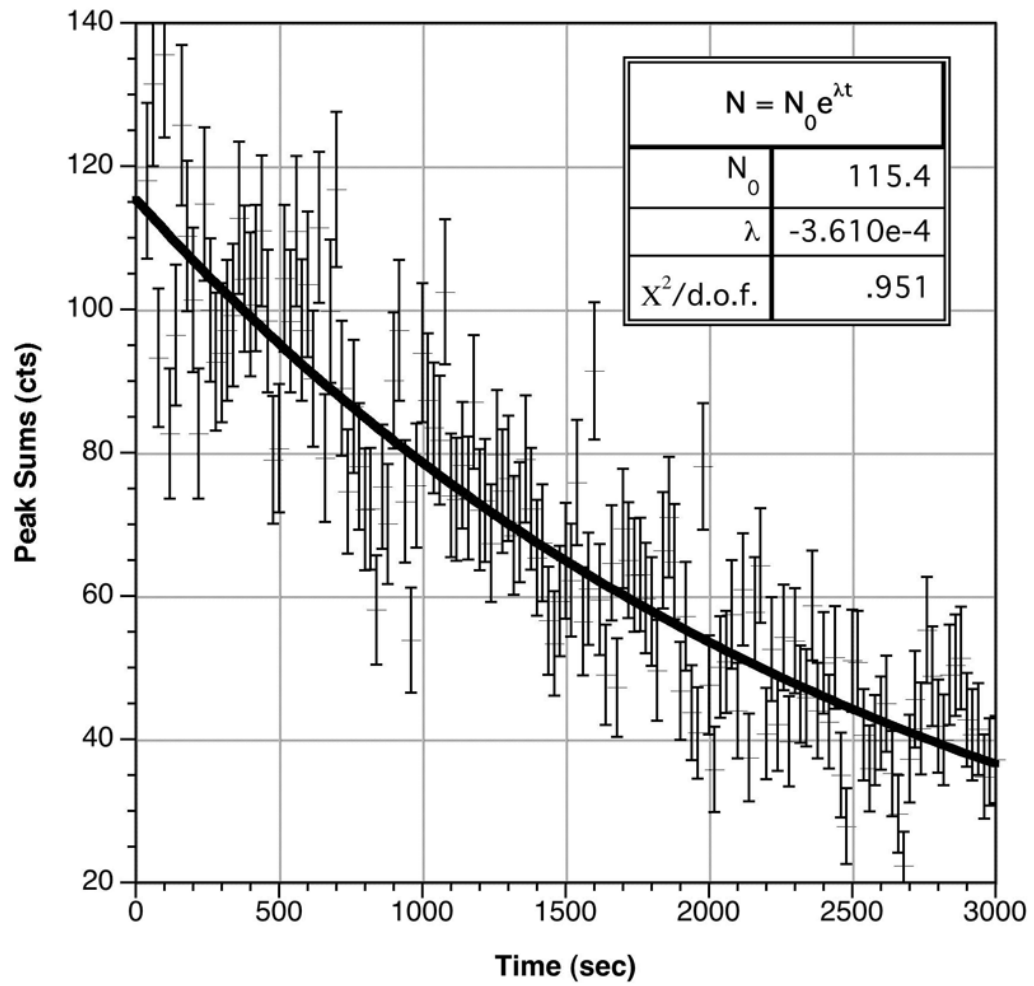Deuteron Energy Loss in 12.5 um aluminum foil as a function of incident energy.

Figure 3.
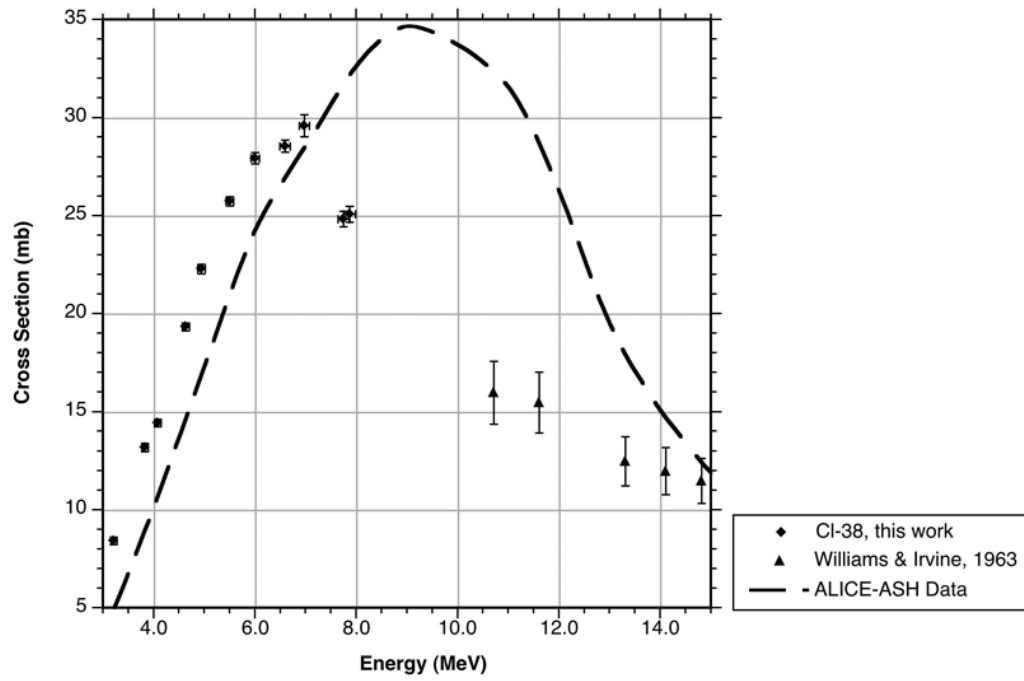Example fit of decay- and pulser-corrected 20 sec peak sums for a single ^{34m}Cl run.

Figure 4.
Measured cross section and statistical error for $^{40}Ar(d,\alpha)^{38}Cl$, including previous work. Eye guide is from ALICE-ASH data.

Figure 5.
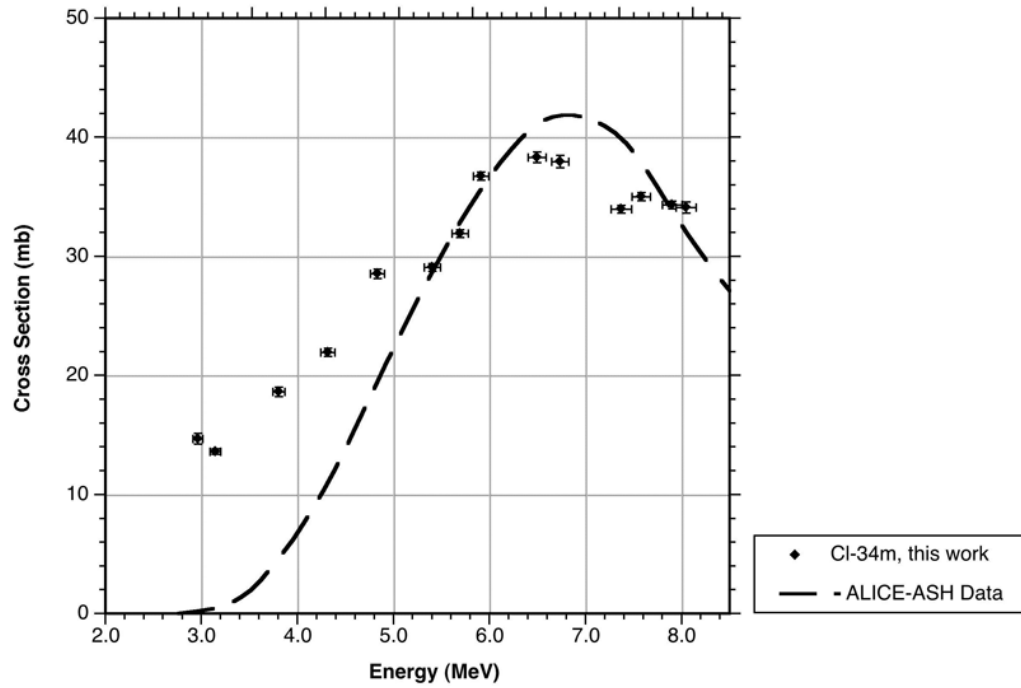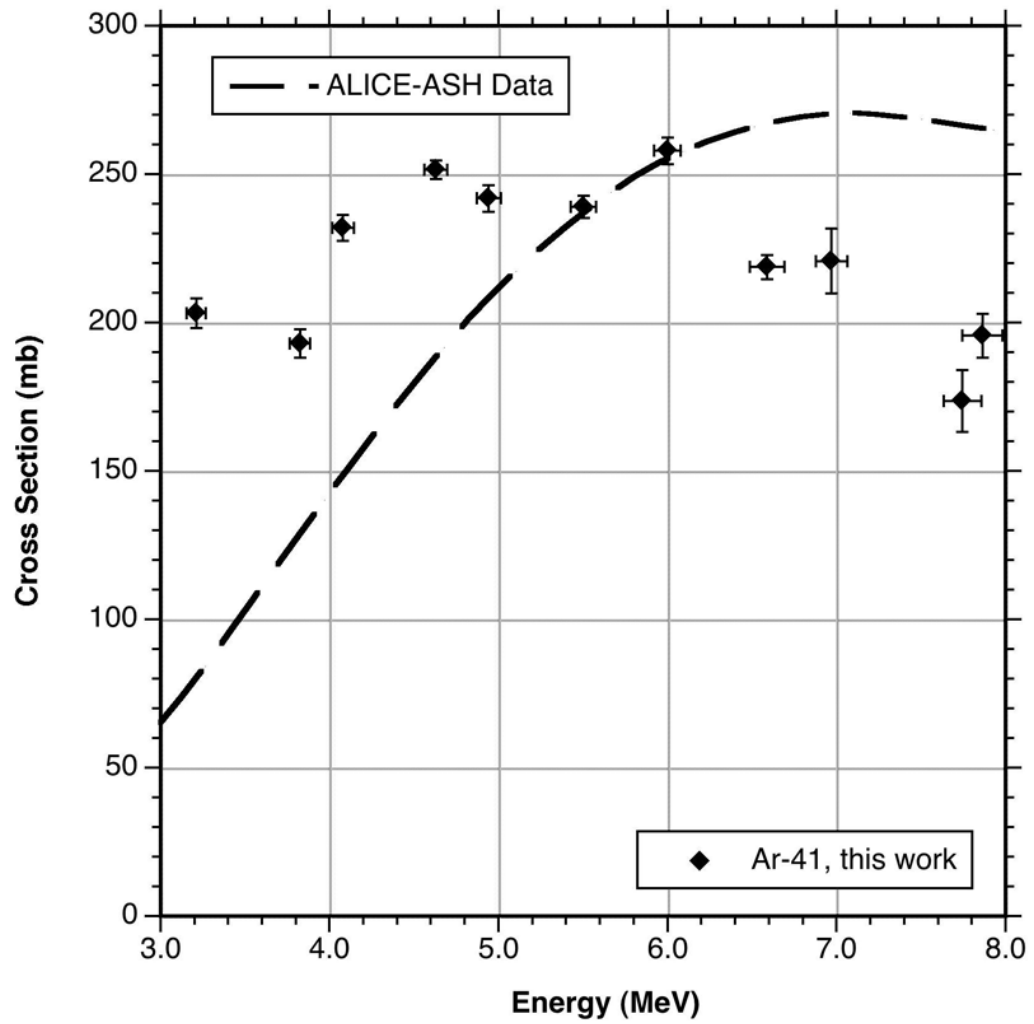Measured cross section and statistical error for $^{36}Ar(d,\alpha)^{34m}Cl$. Eye guide is from ALICE-ASH data.

Figure 6.
Measured cross section and statistical error for $^{40}Ar(d,p)^{41}Ar$. Eye guide is from ALICE-ASH data.

Table 1

Summary of reported excitation function values for production of ^{34m}Cl.

Energy (MeV)	± (MeV)	^{36}Ar(d,α)^{34m}Cl (mb)	± (mb)
2.96	0.05	14.7	0.4
3.14	0.06	13.7	0.2
3.80	0.06	18.7	0.4
4.31	0.07	22.0	0.3
4.83	0.07	28.6	0.4
5.40	0.08	29.2	0.3
5.69	0.08	32.0	0.3
5.91	0.08	36.8	0.3
6.49	0.09	38.4	0.5
6.73	0.09	38.0	0.5
7.37	0.11	34.0	0.3
7.57	0.10	35.1	0.3
7.90	0.10	34.4	0.3

Table 2

Summary of reported excitation function values for production of ^{38}Cl and ^{41}Ar.

Energy (MeV)	± (MeV)	^{40}Ar(d,α)^{38}Cl (mb)	± (mb)	^{40}Ar(d,p)^{41}Ar (mb)	± (mb)
3.20	0.06	8.4	0.2	203.6	5.0
3.82	0.06	13.2	0.2	193.4	4.8
4.07	0.06	14.5	0.2	232.4	4.4
4.62	0.07	19.4	0.2	252.0	3.2
4.94	0.07	22.3	0.2	242.3	4.5
5.49	0.08	25.8	0.2	239.4	3.7
5.99	0.08	28.0	0.3	258.3	4.5
6.58	0.10	28.6	0.3	219.2	4.0
6.96	0.09	29.6	0.6	221.2	10.9
7.74	0.11	24.9	0.4	174.1	10.4
7.86	0.12	25.1	0.4	196.0	7.3